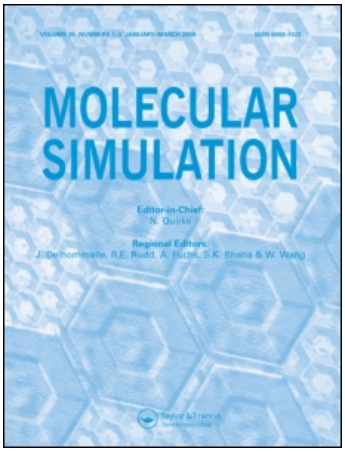

Molecular Simulation
Publication details, including instructions for authors and subscription information:
http://www.informaworld.com/smpp/title~content=t713644482

Folding simulations of three proteins having all α-helix, all β-strand and α/β-structures

Yoshitake Sakae[a]; Yuko Okamoto[a]
[a] Department of Physics, School of Science, Nagoya University, Nagoya, Aichi, Japan

First published on: 10 November 2009

To cite this Article Sakae, Yoshitake and Okamoto, Yuko(2010) 'Folding simulations of three proteins having all α-helix, all β-strand and α/β-structures', Molecular Simulation, 36: 4, 302 — 310, First published on: 10 November 2009 (iFirst)
To link to this Article: DOI: 10.1080/08927020903373638
URL: http://dx.doi.org/10.1080/08927020903373638

Molecular Simulation
Vol. 36, No. 4, April 2010, 302–310

Taylor & Francis
Taylor & Francis Group

Folding simulations of three proteins having all α-helix, all β-strand and α/β-structures

Yoshitake Sakae and Yuko Okamoto*

Department of Physics, School of Science, Nagoya University, Nagoya, Aichi 464-8602, Japan

(*Received 6 April 2009; final version received 29 September 2009*)

We performed folding simulations of three proteins using four force fields, AMBER parm96, AMBER parm99, CHARMM 27 and OPLS-AA/L, in order to examine the features of these force fields. We studied three proteins, protein A (all α-helix), cold-shock protein (all β-strand) and protein G (α/β-structures), for the folding simulations. For the simulation, we used the simulated annealing molecular dynamics method, which was performed 50 times for each protein using the four force fields. The results showed that the secondary-structure-forming tendencies are largely different among the four force fields. AMBER parm96 favours β-bridge structures and extended β-strand structures, and AMBER parm99 favours α-helix structures and 3_{10}-helix structures. CHARMM 27 slightly favours α-helix structures, and there are also π-helix and β-bridge structures. OPLS-AA/L favours α-helix structures and 3_{10}-helix structures.

Keywords: force field; protein; folding simulation; optimisation; secondary structure

1. Introduction

Computational simulations of biomolecular systems are performed using molecular simulation techniques such as Monte Carlo and molecular dynamics (MD) methods. These simulations are usually used within the framework of classical mechanics based on certain potential energy terms with force-field parameters. Potential energy terms and force-field parameters are derived from both experimental results for small molecules and theoretical results using quantum chemistry calculations and MD simulations. Widely used potential energy functions are AMBER [1–3], CHARMM [4], OPLS [5, 6], GROMOS [7] and ECEPP [8]. Recently, detailed comparisons of three versions of AMBER (parm94 [1], parm96 [2] and parm99 [3]), CHARMM [4], OPLS-AA/L [6] and GROMOS [7] have been made by generalised ensemble simulations [9] of two small peptides in an explicit solvent [10,11]. These force fields showed quite different characteristics, especially in secondary-structure-forming tendencies. It was shown that AMBER parm94 is the most (and too much) α-helix-forming among the six force fields studied and that AMBER parm99 and CHARMM give ample amount of α-helix structures, whereas AMBER parm96, OPLS-AA/L and GROMOS are more β-sheet-forming than the rest [10,11]. These results were confirmed by the folding simulations of the two peptides with the implicit solvent model [12–15].

These examinations were performed using two small peptides, C-peptide and G-peptide. The C-peptide is the N-terminal fragment of ribonuclease A and has 13 residues [16,17]. The G-peptide is the C-terminal fragment of the B1 domain of streptococcal protein G and has 16 residues [18–20]. Because these two peptides are smaller than usual proteins, it is desired to examine the differences among the force fields using larger systems.

In this article, we report the results of folding simulations of three proteins that have the representative secondary structures, namely protein A [21] (all α-helix), cold-shock protein [22] (all β-strand) and protein G [23] (α/β-structures). For the simulation, we used the simulated annealing MD method [24], which was performed 50 times with different initial conditions. We compared four of the above force fields, namely AMBER parm96, AMBER parm99, CHARMM 27 and OPLS-AA/L. The results showed that the secondary-structure-forming tendencies of the four force fields were largely different.

In Section 2, the folding simulation method and computational details are described. In Section 3, the results of the simulations are given. In Section 4, the conclusions are given.

2. Materials and methods

Simulated annealing is one of the most widely used global optimisation methods. During a simulated annealing simulation, the temperature is lowered very slowly from a sufficiently high initial temperature to a 'freezing' temperature. If the rate of temperature decrease is slow enough for the system to stay in thermodynamic equilibrium, then it is ensured that the system can avoid getting trapped in states of energy local minima and that the global minimum will be found.

*Corresponding author. Email: okamoto@phys.nagoya-u.ac.jp

ISSN 0892-7022 print/ISSN 1029-0435 online

DOI: 10.1080/08927020903373638
http://www.informaworld.com

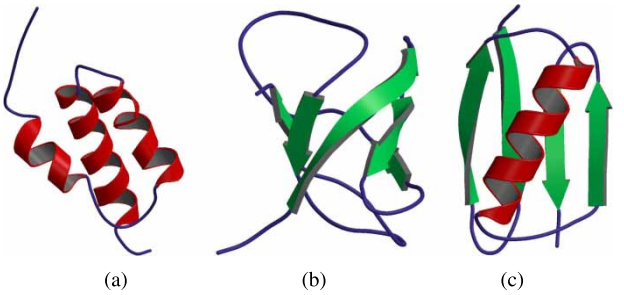

Figure 1. The native structures of the three proteins: (a) protein A, (b) cold-shock protein and (c) protein G. The figures were created with Molscript [32] and Raster3D [33].

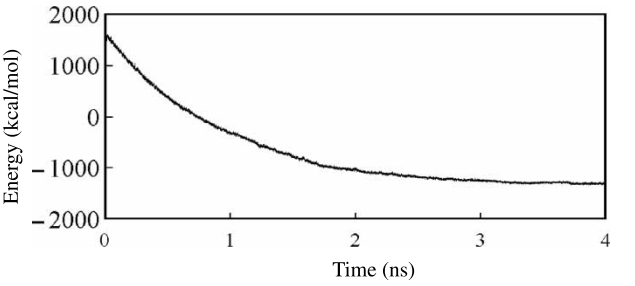

Figure 2. A typical time series of the potential energy during the folding simulation of cold-shock protein using AMBER parm96.

In the present simulation, the temperature was lowered exponentially in N_s MD steps by setting the temperature to

$$T_n = T_I \gamma^{n-1}, \quad (1)$$

for the nth MD step ($n = 1, 2, \ldots, N_S$). Here, T_I is the initial temperature and γ is given by

$$\gamma = \left(\frac{T_F}{T_I}\right)^{1/(N_S-1)}, \quad (2)$$

where T_F is the final temperature. For a fixed value of N_S, these constants (T_I and T_F) are free parameters and have to be tuned in such a way that the annealing process is optimised for the specific problem.

Using the four force fields, we tested their validity by the folding simulations of three proteins: protein A (PDB code: 1BDD) [21], cold-shock protein (PDB code: 3MEF) [22] and protein G (PDB code: 1PGA) [23]. Protein A is a cell wall component of *Staphylococcus aureus* and binds to the portion of immunoglobulin G (IgG) from various mammalian species. The extracellular part of protein A contains five highly homologous domains designated as E, D, A, B and C, each of which is composed of about 60 amino acid residues. We used the B domain in protein A for the folding simulations. The B domain has 60 amino acids and consists of three α-helices, i.e. helix I (Gln10–His19), helix II (Glu25–Asp37) and helix III (Ser42–Ala55) (Figure 1(a)). Cold-shock protein (CspA) from *Escherichia coli* is a single-stranded nucleic acid-binding protein that is produced in response to cold stress. Its precise role in the cell biology of the cold-shock response is yet to be understood. CspA contains 69 amino acids and has five antiparallel β-strands. β-Strands 1–4

Table 1. Number of final conformations with secondary structures obtained from the folding simulations of protein A using the four force fields: AMBER parm96, AMBER parm99, CHARMM 27 and OPLS-AA/L.

	Helix			β-Structure	
	α-Helix	3_{10}-Helix	π-Helix	β-Bridge	Extended β-strand
AMBER parm96	18/50	2/50	1/50	42/50	31/50
AMBER parm99	50/50	49/50	5/50	2/50	0/50
CHARMM 27	33/50	1/50	18/50	25/50	1/50
OPLS-AA/L	24/50	35/50	1/50	19/50	8/50

Notes: The total number of folding simulations in each case was 50. 'α-Helix', '3_{10}-helix', 'π-helix', 'β-bridge' and 'extended β-strand' stand for the number of conformations including the amino acids which were identified by DSSP. Each conformation that has more than one secondary structure is counted multiply.

Table 2. Number of final conformations with secondary structures obtained from the folding simulations of cold-shock protein using the four force fields: AMBER parm96, AMBER parm99, CHARMM 27 and OPLS-AA/L.

	Helix			β-Structure	
	α-Helix	3_{10}-Helix	π-Helix	β-Bridge	Extended β-strand
AMBER parm96	15/50	6/50	1/50	47/50	34/50
AMBER parm99	45/50	50/50	5/50	5/50	1/50
CHARMM 27	28/50	0/50	15/50	38/50	4/50
OPLS-AA/L	20/50	38/50	0/50	36/50	8/50

Note: For description of the terms, see Table 1.

Table 3. Number of final conformations with secondary structures obtained from the folding simulations of protein G using the four force fields: AMBER parm96, AMBER parm99, CHARMM 27 and OPLS-AA/L.

	Helix			β-Structure	
	α-Helix	3_{10}-Helix	π-Helix	β-Bridge	Extended β-strand
AMBER parm96	18/50	1/50	3/50	42/50	31/50
AMBER parm99	50/50	50/50	1/50	1/50	0/50
CHARMM 27	27/50	0/50	19/50	21/50	1/50
OPLS-AA/L	29/50	35/50	1/50	25/50	7/50

Note: For description of the terms, see Table 1.

form a Greek-key topology (Figure 1(b)). Protein G from *Streptococcus* also binds human IgG-like protein A. This protein consists of a series of small binding domains separated by linkers and a cell wall anchor near the C-terminus. Two (in some strains, three) of the domains bind IgG. The IgG-binding domains of protein G are identified as B1, B2, etc. numbering from the N-terminus of the native protein G molecule. We used the B1 domain that consists of a four-stranded β-sheet and an α-helix, and was engineered for production as a 56-residue protein with N-terminal methionine (this position was threonine in the wild type) (Figure 1(c)).

As for force fields, four well-known ones (namely, AMBER parm96, AMBER parm99, CHARMM 27 and OPLS-AA/L) were used. As for solvent effects, we used the generalised-Born/surface area (GB/SA) model [25,26]. We believe that the GB/SA model is good enough for the present purpose, because our previous results of folding simulations of small peptides using the GB/SA model [12–14] agreed very well with those using explicit water molecules [10,11]. Simulated annealing [24] MD simulations were performed from fully extended initial conformations. The unit time step was set to 2.0 fs. Each simulation was carried out for 4 ns (hence, it consisted of 2,000,000 MD steps). The temperature during MD simulations was controlled by Berendsen's method [27]. For each run, the temperature was decreased exponentially from 1200 to 300 K according to Equation (1). We used the program package TINKER version 4.1 (Tinker program package; software available at http://dasher.wustl.edu/tinker/) for all the simulations. For the three proteins, these folding simulations were repeated 50 times with different sets of randomly generated initial velocities.

3. Results and discussion

We now present the results of the folding simulations of the three proteins. In Figure 2, we show a time series of the potential energy of cold-shock protein using AMBER parm96. We see that as the temperature decreases, the potential energy also decreases slowly, suggesting that our simulated annealing runs have been performed properly. As shown in the figure, each run reaches a stable energy value after about 3 ns, which also suggests that no more major conformational change will occur after this. We therefore repeated these runs as many as 50 times starting from different initial conditions, instead of running a single long run.

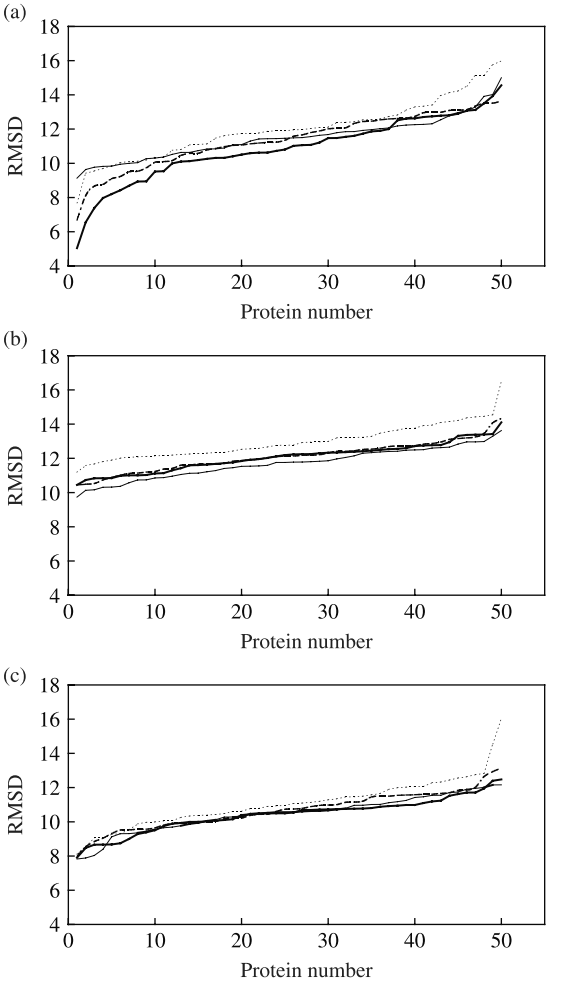

Figure 3. RMSDs of 50 conformations obtained from the folding simulation of (a) protein A, (b) cold-shock protein and (c) protein G, using the four force fields: AMBER parm96 (thin line), AMBER parm99 (thick line), CHARMM 27 (thin dotted line) and OPLS-AA/L (thick dotted line). The conformations are ordered in the increasing order of RMSDs for each case.

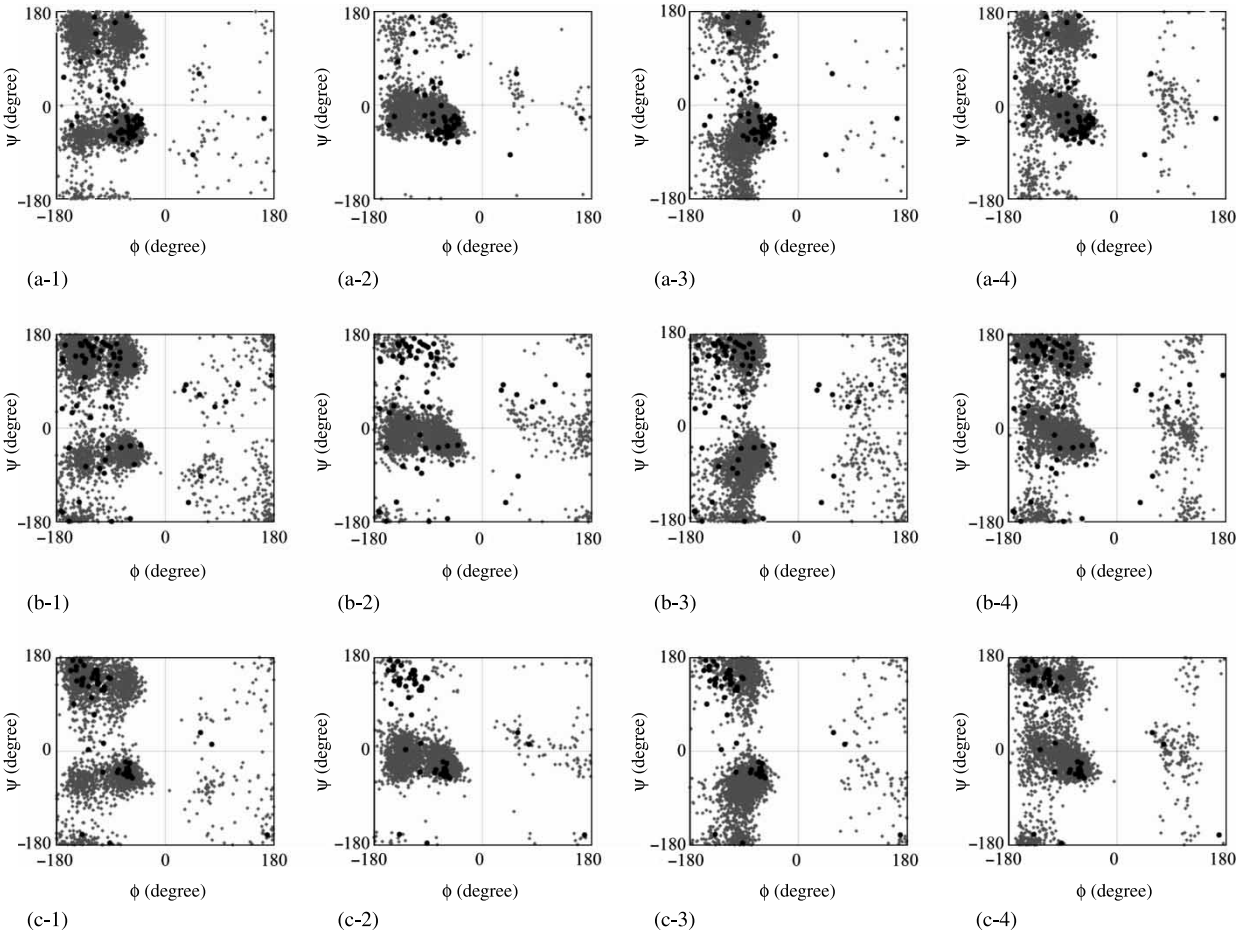

Figure 4. Ramachandran plot of 50 conformations obtained from the folding simulations of (a) protein A, (b) cold-shock protein and (c) protein G, using the four force fields: AMBER parm96 (1), AMBER parm99 (2), CHARMM 27 (3) and OPLS-AA/L (4). Black points are the dihedral angles of the PDB structures.

In Tables 1–3, the number of obtained conformations (final conformations) with helix structures (α-helix, 3_{10}-helix and π-helix) and β-structures (β-bridge, extended β-strand) is listed for the case of protein A, cold-shock protein and protein G, respectively. We used DSSP [28] for the criteria of secondary-structure formations. Table 1 lists the number of final conformations with secondary structures obtained from the folding simulations of protein A using the four force fields: AMBER parm96, AMBER parm99, CHARMM 27 and OPLS-AA/L. Although this result shows that there are some α-helix structures, it confirms that AMBER parm96 favours β-structures more than helix structures in spite of the experimentally determined structures, which are known to consist of three α-helices [21]. AMBER parm99 strongly favours α-helix structures and also favours 3_{10}-helix structures. CHARMM 27 slightly favours α-helix structures, and there are π-helix and β-bridge structures comparatively. Results from a number of recent MD simulations have reported π-helix structures in peptides of varying size and sequence [10,11,29]. OPLS-AA/L favours α-helix structures and 3_{10}-helix structures. The number of 3_{10}-helix structures is more than that of α-helix structures. There are also β-bridge structures.

As for cold-shock protein (Table 2), the results are similar to those in Table 1. However, the number of α-helix structures decreases, and the number of β-bridge and extended β-strand structures increases in comparison with the case of protein A for all force fields except that of extended β-strand structures of OPLS-AA/L. These results show good secondary-structure-forming tendencies because cold-shock protein consists of five antiparallel β-strands [22], namely all β-structures and protein A consist of only three α-helices. Especially, the number of β-bridge structures of CHARMM 27 and OPLS-AA/L increases to 13 conformations and 17 conformations, respectively. As for AMBER parm96 and AMBER parm99, the number of secondary structures changes slightly.

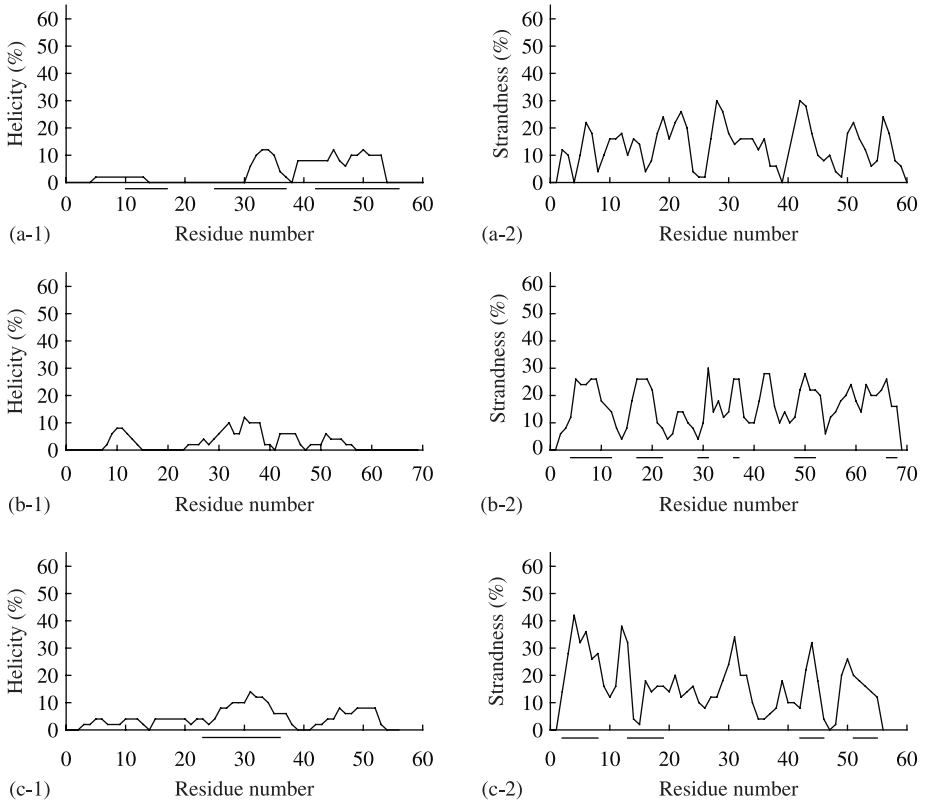

Figure 5. Helicity and strandness as functions of the residue number for [(a-1) and (a-2)] protein A, [(b-1) and (b-2)] cold-shock protein and [(c-1) and (c-2)] protein G. The results are from the final conformations of the 50 simulated annealing runs with AMBER parm96. The underlines show the amino acid residue numbers that have the corresponding secondary structures in the native structures.

As for protein G (Table 3), the results of AMBER parm96 and AMBER parm99 are almost the same as those in Table 1. Protein G consists of a four-stranded β-sheet and a helix. However, we see neither that the number of α-helix structures of protein G clearly increases more than that of cold-shock protein (Table 2) nor that the number of β-structures of protein G increases more than that of protein A (Table 1). As for OPLS-AA/L, there are more number of α-helix structures of protein G than that of cold-shock protein, and there are more number of β-bridge structures of protein G than that of protein A. On the other hand, as for CHARMM 27, the number of secondary structures decreases.

In Figure 3, the root mean square deviations (RMSDs; only backbone atoms except for hydrogen atoms are taken into account) of obtained conformations (final conformations) are plotted for the three proteins. As for protein A, the RMSDs obtained for AMBER parm99 are lower than those for other three force fields, as a whole. Because protein A consists of three α-helix structures and AMBER parm99 favours α-helix structures, this result is reasonable. The first four lowest RMSD conformations for AMBER parm96 have higher RMSDs than those for the other three force fields. This result is consistent with the result that AMBER parm96 does not favour α-helix structures (Table 1). As for cold-shock protein, all the RMSDs for the four force fields are higher than those for the other two proteins. This is because β-sheet structures are usually more difficult to form than α-helix structures. Namely, α-helix structures are based on local interactions, while β-sheet structures are based on non-local interactions along the primary sequence [30]. Moreover, the force fields that we employed in the present work all favour α-helix structures than β-sheet structures except for AMBER parm96 [10–14]. Hence, among the four force fields, the results of the cold-shock protein are the best with AMBER parm96. The RMSDs obtained for AMBER parm96 are slightly lower than those for other three force fields, as a whole. This is because cold-shock protein consists of five antiparallel β-strands and AMBER parm96 favours β-structures (Table 2). In the case of protein G, we cannot see major difference among the four force fields. The lowest RMSDs of the four force fields, AMBER parm96, AMBER parm99, OPLS-AA/L and CHARMM 27, are 7.82, 7.91, 8.01 and 8.10, respectively. In comparison with RMSDs of protein A and cold-shock

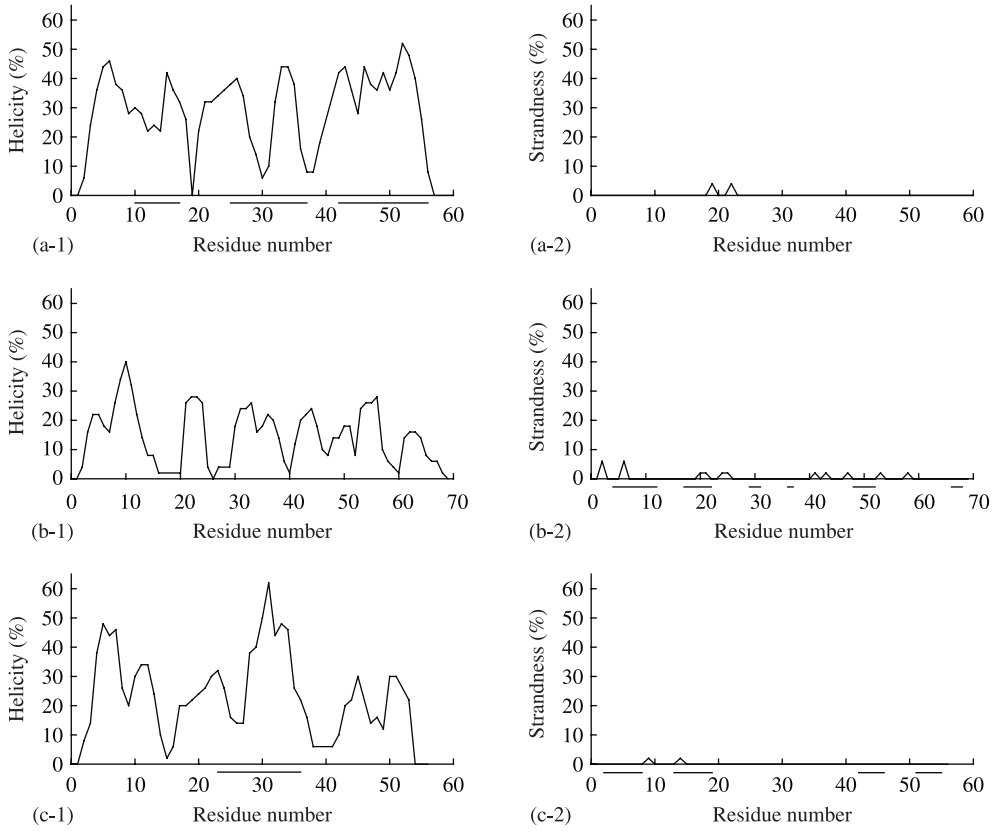

Figure 6. [(a-1), (b-1) and (c-1)] Helicity and [(a-2), (b-2) and (c-2)] strandness for each residue of [(a-1) and (a-2)] protein A, [(b-1) and (b-2)] cold-shock protein and [(c-1) and (c-2)] protein G, using AMBER parm99. See also the caption of Figure 5.

protein, those of protein G have a little difference among the four force fields. As a whole, we see that the RMSDs obtained from the conformations of CHARMM 27 for the three proteins are higher than those for the other force fields.

In Figure 4, we show the Ramachandran plots of the 50 final conformations obtained from the folding simulations of the three proteins. We see that there are many backbone dihedral angles around the α-helix region (−57°, −47°) or parallel β-sheet region (−119°, 113°) and antiparallel β-sheet region (−139°, 135°) for all force fields [31]. As for AMBER parm99, many points of backbone dihedral angles are clearly concentrated around the α-helix region (−57°, −47°). As for AMBER parm96, the backbone dihedral angles are distributed around the parallel β-sheet region (−119°, 113°) and antiparallel β-sheet region (−139°, 135°) more than the α-helix region. Although the difference in distributions of the backbone dihedral angles among the four force fields is clear, the difference in distributions among the three proteins is not clear. Namely, this result shows that the secondary-structure-forming tendencies depend on the difference in force fields greatly.

In Figures 5–8, we show the helicity and the strandness as functions of residue numbers. As for AMBER parm96 (Figure 5), as a whole, the helicity is lower than the strandness for all three proteins. The helicity of the 10–17 and 25–30 regions of protein A has a low percentage at the region of amino acid sequence, which is known as α-helix structure. However, the helicities of the 31–37 and 42–53 regions of protein A and of the 23–36 region of protein G have some percentage (2–14%) at the α-helix region of the native structures. The strandness of cold-shock protein and protein G has a high percentage at the β-sheet region of the native structures; however, the 14–15 region of amino acid sequence (–Gly–Glu–) of protein G has lower strandness than the other β-sheet region. We see that the number of amino acids, which have high helicity, clearly increases for AMBER parm99 (Figure 6), and the strandness has a little percentage for all three proteins. However, helicities of the 28–31 region of amino acid sequence (–Arg–Asn–Gly–) of protein A and of the 25–27 region of amino acid sequence (–Thr–Ala–Glu–) of protein G are low in spite of these regions being α-helix regions at the native structures. As for CHARMM 27 (Figure 7), as a whole, the helicities are higher than the strandness for all three proteins. However, the 12–15 region of amino acid sequence

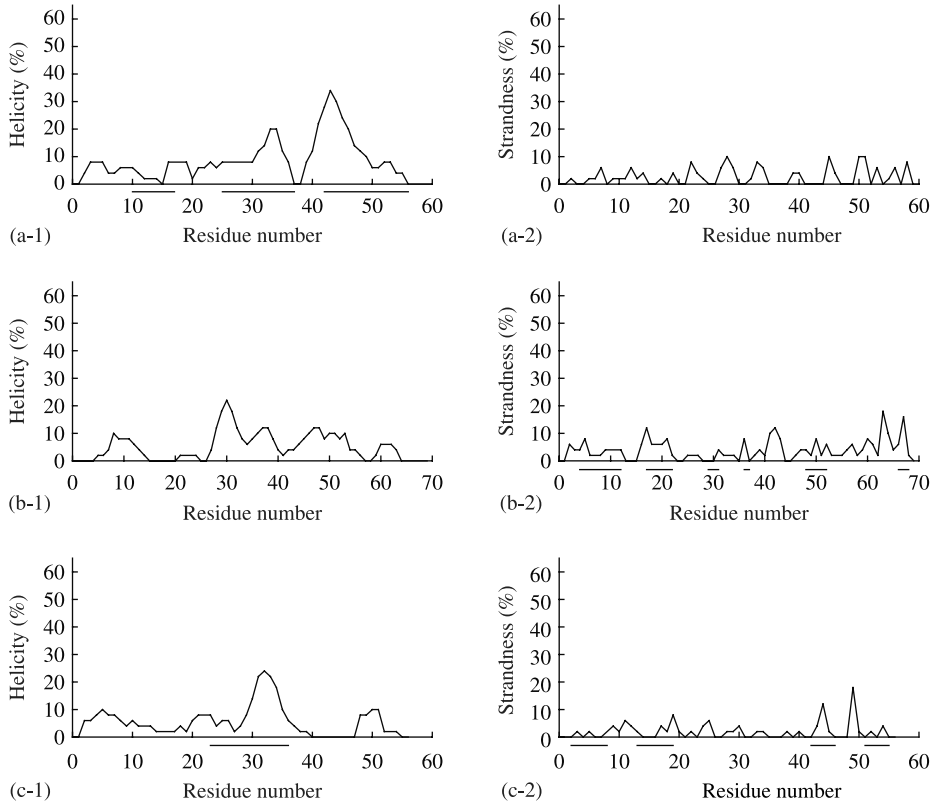

Figure 7. [(a-1), (b-1) and (c-1)] Helicity and [(a-2), (b-2) and (c-2)] strandness for each residue of [(a-1) and (a-2)] protein A, [(b-1) and (b-2)] cold-shock protein and [(c-1) and (c-2)] protein G, using CHARMM 27. See also the caption of Figure 5.

(–Asn–Ala–Phe–Tyr–) of protein A and Glu27 of protein G have low helicity. Although we see some β-bridge formations in the regions that correspond to the native β-strands, overall preferences are still α-helical for CHARMM 27. As for OPLS-AA/L (Figure 8), the average of the helicity is the same as that of the strandness for all three proteins. As for OPLS-AA/L, the helicity has a high percentage at the 42–56 region of amino acid sequence of protein A. Although the strandness of OPLS-AA/L is about 10% for some regions of native structures, the 49–52 region of amino acid sequence (–Lys–Val–Ser–Phe–) of cold-shock protein and the 14–19 region of amino acid sequence (–Gly–Glu–Thr–Thr–Thr–Glu–) of protein G have lower strandness than the other β-sheet regions. These results suggest that force-field parameters for some amino acids, especially Gly and some polar amino acids, do not represent the secondary structures of the native structures correctly.

4. Conclusions

In this article, we present the results of the folding simulations of three proteins using four force fields, AMBER parm96, AMBER parm99, CHARMM 27 and OPLS-AA/L. For these simulations, we used three proteins, which have typical secondary structures, namely protein A (all α-helix), cold-shock protein (all β-strand) and protein G (α/β). For the simulation, we used the simulated annealing molecular dynamics method, which was performed 50 times for each protein with the four force fields. Although we did not observe folding into native structures, perhaps due to insufficient computational time, we could still examine the secondary-structure-forming tendencies of the four force fields. We indeed found that the secondary-structure-forming tendencies of the four force fields are largely different. AMBER parm96 favours β-structures, and AMBER parm99 favours α-helix and 3_{10}-helix structures. CHARMM 27 slightly favours α-helix structures and there are π-helix and β-bridge structures comparatively. OPLS-AA/L favours α-helix structures and 3_{10}-helix structures, and the 3_{10}-helix structures are favoured more than α-helix structures. Additionally, there are β-bridge structures comparatively. These secondary-structure-forming tendencies are similar among the three proteins and depend on the difference in force fields strongly.

Moreover, we examined the helicity and the strandness as functions of residue numbers of the three proteins. These results show that force-field parameters for some amino acids, especially Gly and some polar amino acids, do not represent the secondary structures of

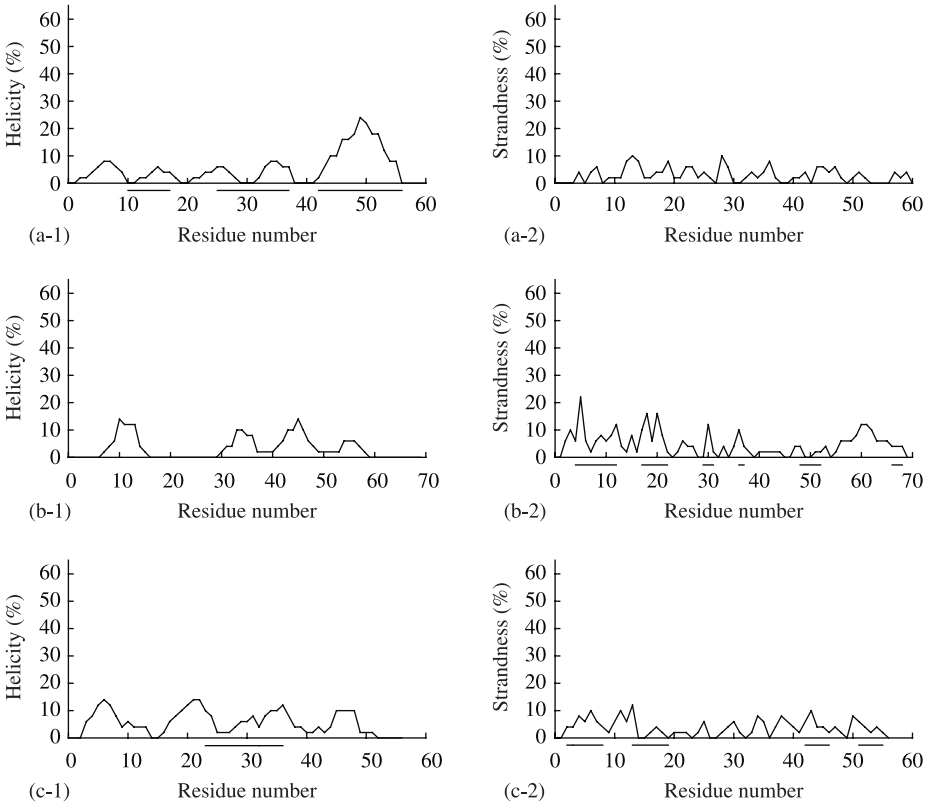

Figure 8. [(a-1), (b-1) and (c-1)] Helicity and [(a-2), (b-2) and (c-2)] strandness for each residue of [(a-1) and (a-2)] protein A, [(b-1) and (b-2)] cold-shock protein and [(c-1) and (c-2)] protein G, using OPLS-AA/L. See also the caption of Figure 5.

the native structures correctly. By taking into account the results of the present work, we should improve the existing force fields.

Acknowledgements

The computations were performed on SuperNOVA of Miki Laboratory at Doshisha University and on the computers at the Research Center for Computational Science, Institute for Molecular Science. This work was supported, in part, by the Grants-in-Aid for the Academic Frontier Project, 'Intelligent Information Science', for the Nano-Bio-IT Education Program, for Scientific Research on Innovative Areas ('Fluctuations and Biological Functions'), and for the Next Generation Super Computing Project, Nanoscience Program from the Ministry of Education, Culture, Sports, Science and Technology (MEXT), Japan.

References

[1] W.D. Cornell, P. Cieplak, C.I. Bayly, I.R. Gould, J. Kenneth, M. Merz, D.M. Ferguson, D.C. Spellmeyer, T. Fox, J.W. Caldwell, and P.A. Kollman, *A second generation force field for the simulation of proteins, nucleic acids, and organic molecules*, J. Am. Chem. Soc. 117 (1995), pp. 5179–5197.

[2] P.A. Kollman, R. Dixon, W. Cornell, T. Fox, C. Chipot, and A. Pohorille, *The development/application of a 'minimalist' organic/biochemical molecular mechanic force field using a combination of* ab initio *calculations and experimental data*, in *Computer Simulations of Biological Systems*, ESCOM, Dordrecht, 1997, pp. 83–96.

[3] J. Wang, P. Cieplak, and P.A. Kollman, *How well does a restrained electrostatic potential (RESP) model perform in calculating conformational energies of organic and biological molecules?* J. Comput. Chem. 21 (2000), pp. 1049–1074.

[4] A.D. MacKerell Jr., D. Bashford, M. Bellott, R.L. Dunbrack Jr., J.D. Evanseck, M.J. Field, S. Fischer, J. Gao, H. Guo, S. Ha, D. Joseph-McCarthy, L. Kuchnir, K. Kuczera, F.T.K. Lau, C. Mattos, S. Michnick, T. Ngo, D.T. Nguyen, B. Prodhom, W.E. Reiher III, B. Roux, M. Schlenkrich, J.C. Smith, R. Stote, J. Straub, M. Watanabe, J. Wiorkiewicz-Kuczera, D. Yin, and M. Karplus, *All-atom empirical potential for molecular modeling and dynamics studies of proteins*, J. Phys. Chem. B 102 (1998), pp. 3586–3616.

[5] W.L. Jorgensen, D.S. Maxwell, and J. Tirado-Rives, *Development and testing of the OPLS all-atom force field on conformational energetics and properties of organic liquids*, J. Am. Chem. Soc. 118 (1996), pp. 11225–11236.

[6] G.A. Kaminski, R.A. Friesner, J. Tirado-Rives, and W.L. Jorgensen, *Evaluation and reparametrization of the OPLS-AA force field for proteins via comparison with accurate quantum chemical calculations on peptides*, J. Phys. Chem. B 105 (2001), pp. 6474–6487.

[7] W.F. Gunsteren, S.R. Billeter, A.A. Eising, P.H. Hünenberger, P. Krüger, A.E. Mark, W.R.P. Scott, and I.G. Tironi, *Biomolecular Simulation: The GROMOS96 Manual and User Guide*, Vdf Hochschulverlag AG an der ETH Zürich, Zürich, 1996.

[8] G. Némethy, K.D. Gibson, K.A. Palmer, C.N. Yoon, G. Paterlini, A. Zagari, S. Rumsey, and H. Scheraga, *Energy parameters in polypeptides. 10. Improved geometrical parameters and nonbonded interactions for use in the ECEPP/3 algorithm, with application to proline-containing peptides*, J. Phys. Chem. 96 (1992), pp. 6472–6484.

[9] A. Mitsutake, Y. Sugita, and Y. Okamoto, *Generalized-ensemble algorithms for molecular simulations of biopolymers*, Biopolymers (Pept. Sci.) 60 (2001), pp. 96–123.
[10] T. Yoda, Y. Sugita, and Y. Okamoto, *Comparisons of force fields for proteins by generalized-ensemble simulations*, Chem. Phys. Lett. 386 (2004), pp. 460–467.
[11] T. Yoda, Y. Sugita, and Y. Okamoto, *Secondary-structure preferences of force fields for proteins evaluated by generalized-ensemble simulations*, Chem. Phys. 307 (2004), pp. 269–283.
[12] Y. Sakae and Y. Okamoto, *Optimization of protein force-field parameters with the Protein Data Bank*, Chem. Phys. Lett. 382 (2003), pp. 626–636.
[13] Y. Sakae and Y. Okamoto, *Protein force-field parameters optimized with the Protein Data Bank. I. Force-field optimizations*, J. Theor. Comput. Chem. 3 (2004), pp. 339–358.
[14] Y. Sakae and Y. Okamoto, *Protein force-field parameters optimized with the Protein Data Bank. II. Comparisons of force fields by folding simulations of short peptides*, J. Theor. Comput. Chem. 3 (2004), pp. 359–378.
[15] Y. Sakae and Y. Okamoto, *Secondary-structure design of proteins by a backbone torsion energy*, J. Phys. Soc. Jpn. 75 (2006), 054802 (9 pages).
[16] K.R. Shoemaker, P.S. Kim, D.N. Brems, S. Marqusee, E.J. York, I.M. Chaiken, J.M. Stewart, and R.L. Baldwin, *Nature of the charged-group effect on the stability of the C-peptide helix*, Proc. Natl Acad. Sci. USA 82 (1985), pp. 2349–2353.
[17] J.J. Osterhout Jr., R.L. Baldwin, E.J. York, J.M. Stewart, H.J. Dyson, and P.E. Wright, *^{1}H NMR studies of the solution conformations of an analogue of the C-peptide of ribonuclease A*, Biochemistry 28 (1989), pp. 7059–7064.
[18] F.J. Blanco, G. Rivas, and L. Serrano, *A short linear peptide that folds into a native stable bold beta-hairpin in aqueous solution*, Nature Struct. Biol. 1 (1994), pp. 584–590.
[19] N. Kobayashi, S. Honda, H. Yoshii, H. Uedaira, and E. Munekata, *Complement assembly of two fragments of the streptococcal protein G B1 domain in aqueous solution*, FEBS Lett. 366 (1995), pp. 99–103.
[20] S. Honda, N. Kobayashi, and E. Munekata, *Thermodynamics of a β-hairpin structure: Evidence for cooperative formation of folding nucleus*, J. Mol. Biol. 295 (2000), pp. 269–278.
[21] H. Gouda, H. Torigoe, A. Saito, M. Sato, Y. Arata, and I. Shimada, *Three-dimensional solution structure of the B domain of staphylococcal protein A: Comparisons of the solution and crystal structures*, Biochemistry 31 (1992), pp. 9665–9672.
[22] W. Feng, R. Tejero, D.E. Zimmerman, M. Inouye, and G.T. Montelione, *Solution NMR structure and backbone dynamics of the major cold-shock protein (CspA) from* Escherichia coli*: Evidence for conformational dynamics in the single-stranded RNA-binding site*, Biochemistry 37 (1998), pp. 10881–10896.
[23] T. Gallagher, P. Alexander, P. Bryan, and G.L. Gilliland, *Two crystal structures of the B1 immunoglobulin-binding domain of streptococcal protein G and comparison with NMR*, Biochemistry 33 (1994), pp. 4721–4729.
[24] S. Kirkpatrick, C.D. Gelatt Jr., and M.P. Vecchi, *Optimization by simulated annealing*, Science 220 (1983), pp. 671–680.
[25] W.C. Still, A. Tempczyk, R.C. Hawley, and T. Hendrickson, *Semianalytical treatment of solvation for molecular mechanics and dynamics*, J. Am. Chem. Soc. 112 (1990), pp. 6127–6129.
[26] D. Qiu, P.S. Shenkin, F.P. Hollinger, and W.C. Still, *The GB/SA continuum model for solvation. A fast analytical method for the calculation of approximate born radii*, J. Phys. Chem. A 101 (1990), pp. 3005–3014.
[27] H.J.C. Berendsen, J.P.M. Postma, W.F. Gunsteren, A. DiNola, and J.R. Haak, *Molecular dynamics with coupling to an external bath*, J. Chem. Phys. 81 (1984), pp. 3684–3690.
[28] W. Kabsch and C. Sander, *Dictionary of protein secondary structure: Pattern recognition of hydrogen-bonded and geometrical features*, Biopolymers 22 (1983), pp. 2577–2637.
[29] M. Feig, A.D. MacKerell, and C.L. Brooks III, *Force field influence on the observation of π-helical protein structures in molecular dynamics simulations*, J. Phys. Chem. B 107 (2003), pp. 2831–2836.
[30] D. Baker, *A surprising simplicity to protein folding*, Nature 405 (2000), pp. 39–42.
[31] G.N. Ramachandran and V. Sasisekharan, *Conformation of polypeptides and proteins*, Adv. Protein Chem. 23 (1968), pp. 283–438.
[32] P.J. Kraulis, *MOLSCRIPT: A program to produce both detailed and schematic plots of protein structures*, J. Appl. Cryst. 24 (1991), pp. 946–950.
[33] E.A. Merritt and D.J. Bacon, *Raster3D: Photorealistic molecular graphics*, Methods Enzymol. 277 (1997), pp. 505–524.